

Towards end-to-end LLM-based censoring-aware survival analysis

Yishu Wei, Ph.D.^{1,†}, Hexin Dong, Ph.D.^{1,†}, Yi Lin, Ph.D.¹, Jiahe Qian, M.S.¹, Yi Liu, M.D.², and Yifan Peng, Ph.D.^{1,*}

¹Department of Population Health Science, Weill Cornell Medicine, New York, 10065, US

²Department of Medicine, Weill Cornell Medicine, New York, 10065, US

[†]These authors contributed equally to this work.

*Corresponding author(s). Email(s): yip4002@med.cornell.edu

Abstract

Objective: Survival analysis is central to medical prediction, yet large language models (LLMs) are rarely used as end-to-end survival models because censoring prevents straightforward supervised fine-tuning. Here we present LLMSurvival, a framework that enables censoring-aware survival analysis with unmodified LLMs operating directly on tabular clinical data.

Materials and Methods: LLMSurvival reformulates time-to-event prediction as pairwise ranking among comparable subjects, and derives test-time risk by aggregating comparisons against anchor individuals from the training cohort.

Results: Across two clinical tasks (ICU mortality prediction in MIMIC-IV and fragility fracture prediction in a NewYork-Presbyterian/Weill Cornell Medicine cohort), LLMSurvival improves overall concordance over Cox proportional hazards modeling by 3.1% for ICU mortality and 0.5% for fracture risk, 2.1% on average for ICU mortality and 2.8% for fracture risk over three established deep learning survival models.

Discussion: The results show that survival modeling with censoring can be made compatible with LLM fine-tuning through comparison-based reformulation. The framework demonstrates high portability and superior performance over expert curated scores like SAPS-II and FRAX scores across diverse clinical context. Furthermore, the framework supports local deployment, as compact, publicly available base models provide sufficient performance.

Conclusion: The LLMSurvival framework serves as a proof of concept for an integrated, censoring-conscious approach to survival analysis via LLMs.

Keywords: Large Language Models, Survival Analysis, Prognosis, Machine Learning, Clinical Decision Support Systems

1 BACKGROUND AND SIGNIFICANCE

Survival analysis is a central problem in statistics and machine learning, particularly within the medical domain. Its objective is to model not only whether an event will occur but also the time until its occurrence [1]. Although extensive research has explored the application of LLMs to survival analysis, the majority of these studies utilize LLMs merely as feature extractors rather than direct predictive models, or require substantial architectural modifications [2]. Shahid et al. [3] used an LLM as a feature extractor to obtain variables from clinical notes. Vaidyanathan et al. [4] simplified the survival analysis problem into a five-year classification task and did not address censoring. Wen et al. [5] also used an LLM to extract features for a survival model. Steinberg et al. [6] used a piecewise-exponential artificial neural network to predict the hazard rate. Similarly, Esteban et al. [7] added dedicated neural networks on top of an LLM and experimented with ordinal

regression loss and discordant pair loss. When neural networks are added on top of an LLM, the LLMs still serve primarily as feature extractors. For a summary of the previous literature, please refer to eTable 1 in Supplement 1.

Large language models (LLMs) have been directly employed as end-to-end models for classical statistical learning tasks without architectural modifications. For instance, Dinh et al. [8] formatted a regression task on tabular data into natural language prompts. They used the template “When we have $x_1 = r.x1, x_2 = r.x2, \dots, x_p = r.xp$, what should be y ? ### $y = r.y @@@$ ” to format data and fine-tune LLM based on that. Similarly, Hegselmann et al. [9] fine-tuned LLMs for classification by framing problems as binary “Yes/No” questions, achieving performance comparable to traditional statistical methods. However, such strategies cannot be readily extended to survival analysis due to the challenges of censoring. Censoring occurs when the exact time of an event is unknown, typically because a subject withdraws from a study or the observation period concludes before the event occurs. Discarding censored subjects introduces significant bias [10]. Conversely, including them is difficult because they lack explicit labels. This lack of ground truth poses a fundamental hurdle for LLM training, particularly in the widely adopted supervised fine-tuning and reinforcement learning frameworks.

In this study, we aim to bridge a gap in the literature and address the challenge that LLMs cannot be directly optimized for survival analysis due to the lack of explicit labels caused by censoring. We present LLMSurvival, a multi-stage framework designed to apply LLMs to survival analysis directly on tabular data. Rather than training the LLM to directly predict survival times, we optimize the model for pairwise comparison. During inference, each subject is compared against a set of pre-selected anchor subjects. The risk score is then estimated based on the proportion of comparisons in which the test subject is predicted to experience the event earlier. By reformulating survival analysis as a ranking problem, we naturally circumvent the challenges of censoring and can use all comparable pairs. Furthermore, this ranking approach leverages the inherent strengths of LLMs, as comparing two subject profiles described in natural language is a task well-suited to their contextual reasoning.

Treating survival analysis as a ranking problem has been widely explored in prior machine learning and deep learning work [11–14]. However, there is limited research extending these explorations to large language models. LLMs have independently shown strong performance on ranking tasks in natural language processing [15, 16]. Our work bridges these two lines of research. Pairwise ranking effectively addresses censoring while leveraging LLMs’ inherent strengths, positioning this approach at the ideal intersection of survival analysis and natural language processing.

We evaluate LLMSurvival in two diverse clinically important applications: mortality prediction in the Intensive Care Unit (ICU) and fracture risk assessment. Across both settings, LLMSurvival achieves performance that is better than traditional and deep-learning-based survival methods (e.g., Cox proportional hazards model, Cox-nnet [17], Deephit [18] and DeepSurv [19]). Furthermore, the model outperforms established clinical risk scores, including SAPS II for ICU mortality and FRAX for fracture risk. LLMSurvival also exhibits consistent performance trends across follow-up intervals.

The main contribution of this study is to introduce a framework that can directly train an LLM as the modeler for survival analysis. It expands its role from mere feature extractors or bottom layers of the overall architecture to a comprehensive, end-to-end modeling pipeline. It serves as a proof of concept, demonstrating that large language models can expand their capabilities to solve more complex statistical problems on their own. In addition, it demonstrates that reformulating a complex problem (such as survival analysis) into a task better suited to LLMs (e.g., pairwise comparison) enables them to tackle challenges they could not otherwise solve independently.

2 MATERIALS AND METHODS

2.1 Ethics statement

The retrospective analysis of internal electronic medical records was reviewed and approved by the Weill Cornell Medicine Institutional Review Board. All data were anonymized before computational analysis. Because the study used retrospective de-identified data and involved no direct patient contact, informed consent was waived.

2.2 Study design

We evaluated LLMSurvival on two complementary cohorts representing acute and chronic clinical prediction tasks: ICU mortality prediction using MIMIC-ICU (Table 1) and incident fragility fracture prediction using an NYP/WCM cohort (Table 2). For both cohorts, data were split into training and test sets in an 8:2 ratio.

MIMIC-ICU cohort. We used MIMIC-IV (Medical Information Mart for Intensive Care IV) [20], a de-identified electronic health record database of adult ICU admissions at Beth Israel Deaconess Medical Center between 2008 and 2019. For consistency with previous work, we adopted the cohort definition of Lin et al. [21], yielding 9,928 ICU patients. Of these, 2,213 (22%) deceased during their ICU stay (Table 1).

We used SAPS-II-based structured variables derived from the first ICU day, including age, physiologic measures, laboratory abnormalities, chronic disease burden, and admission type [22]. SAPS-II scores were computed according to the original definition using publicly available code¹.

Table 1: Participant demographic and clinical characteristics on the MIMIC-ICU cohort.

Characteristic	Participants, No. (%)		
	All (N=9928)	Discharge (n=7715)	Mortality (n=2213)
Age, mean (SD), y	65.13 (17.99)	63.32 (18.38)	71.43 (14.93)
Gender, male/female, %	5416 (55) / 4512 (45)	4221 (55) / 3494 (45)	1195 (54) / 1018 (46)
SAPS-II, mean (SD)	37.25 (15.44)	33.51 (13.01)	50.29 (16.15)
SAPS-II physiological measurements			
Age, year			
< 40	1036 (10.44)	965 (12.51)	71 (3.21)
40-59	2390 (24.07)	1999 (25.91)	391 (17.67)
60-69	2127 (21.42)	1669 (21.63)	458 (20.70)
70-74	969 (9.76)	707 (9.16)	262 (11.84)
75-79	957 (9.64)	709 (9.19)	248 (11.21)
≥ 80	2449 (24.67)	1666 (21.59)	783 (35.38)
Heart Rate			
< 40	187 (1.88)	80 (1.04)	107 (4.84)
40-69	3884 (39.12)	3262 (42.28)	622 (28.11)
70-119	3406 (34.31)	2678 (34.71)	728 (32.90)

Continued on next page

¹<https://github.com/MIT-LCP/mimic-code/blob/main/mimic-iii/concepts/severityscores/sapsii.sql>

Table 1: Participant demographic and clinical characteristics on the MIMIC-ICU cohort. (Continued)

Characteristic	Participants, No. (%)		
	All (N=9928)	Discharge (n=7715)	Mortality (n=2213)
120-159	2314 (23.31)	1623 (21.04)	691 (31.22)
≥ 160	137 (1.38)	72 (0.93)	65 (2.94)
Systolic BP, mmHg			
< 70	912 (9.19)	425 (5.51)	487 (22.01)
70-99	6138 (61.83)	4821 (62.49)	1317 (59.51)
100-199	2764 (27.84)	2378 (30.82)	386 (17.44)
≥ 200	114 (1.15)	91 (1.18)	23 (1.04)
Temperature ≤ 39 °C			
No	9449 (95.18)	7374 (95.58)	2075 (93.76)
Yes	479 (4.82)	341 (4.42)	138 (6.24)
PaO ₂ / FiO ₂ , mmHg			
< 100	562 (5.66)	268 (3.47)	294 (13.29)
100-199	892 (8.98)	584 (7.57)	308 (13.92)
≥ 200	1439 (14.49)	1054 (13.66)	385 (17.40)
No ventilation	7035 (70.86)	5809 (75.29)	1226 (55.40)
Blood urea nitrogen, mg/dL			
< 28	6471 (65.18)	5422 (70.28)	1049 (47.40)
28-93	3090 (31.12)	2068 (26.80)	1022 (46.18)
≥ 84	367 (3.70)	225 (2.92)	142 (6.42)
Urine output, mL/day			
< 500	1246 (12.55)	591 (7.66)	655 (29.60)
500-999	1738 (17.51)	1299 (16.84)	439 (19.84)
≥ 1000	6944 (69.94)	5825 (75.50)	1119 (50.56)
Sodium, mEq/L			
< 125	227 (2.29)	170 (2.20)	57 (2.58)
125-144	8686 (87.49)	6890 (89.31)	1796 (81.16)
≥ 145	1015 (10.22)	655 (8.49)	360 (16.27)
Potassium			
3.0-4.9	7898 (79.55)	6350 (82.31)	1548 (69.95)
< 3.0 or ≥ 5.0	2030 (20.45)	1365 (17.69)	665 (30.05)
Bicarbonate, mEq/L			
< 15	729 (7.34)	364 (4.72)	365 (16.49)
15-19	1977 (19.91)	1396 (18.09)	581 (26.25)
≥ 20	7222 (72.74)	5955 (77.19)	1267 (57.25)
Bilirubin, mg/dL			
< 4.0	9453 (95.22)	7456 (96.64)	1997 (90.24)
4.0-5.9	157 (1.58)	96 (1.24)	61 (2.76)
≥ 6.0	318 (3.20)	163 (2.11)	155 (7.00)

Continued on next page

Table 1: Participant demographic and clinical characteristics on the MIMIC-ICU cohort. (Continued)

Characteristic	Participants, No. (%)		
	All (N=9928)	Discharge (n=7715)	Mortality (n=2213)
White blood count, $\times 10^3/\text{mm}^3$			
< 1.0	81 (0.82)	35 (0.45)	46 (2.08)
1.0-19.9	8602 (86.64)	6896 (89.38)	1706 (77.09)
≥ 20.0	1245 (12.54)	784 (10.16)	461 (20.83)
Glasgow coma scale			
14-15	7590 (76.45)	6072 (78.70)	1518 (68.59)
11-13	1142 (11.50)	900 (11.67)	242 (10.94)
9-10	406 (4.09)	285 (3.69)	121 (5.47)
6-8	455 (4.58)	297 (3.85)	158 (7.14)
< 6	335 (3.37)	161 (2.09)	174 (7.86)
Chronic disease			
None	8682 (87.45)	6987 (90.56)	1695 (76.59)
Metastatic cancer	820 (8.26)	473 (6.13)	347 (15.68)
Hematologic malignancy	341 (3.43)	185 (2.40)	156 (7.05)
AIDS	85 (0.86)	70 (0.91)	15 (0.68)
Type of admission			
Scheduled surgical	60 (0.60)	58 (0.75)	2 (0.09)
Medical	8358 (84.19)	6442 (83.50)	1916 (86.58)
Unscheduled surgical	1510 (15.21)	1215 (15.75)	295 (13.33)

NYP/WCM fracture cohort. We assembled a retrospective cohort from NewYork-Presbyterian/Weill Cornell Medicine electronic health records (Table 2). Eligible patients were aged 50 years or older, underwent at least one DXA scan between January 1, 2012 and September 3, 2025, and had at least two years of follow-up. Demographics, prior fracture status, comorbidities, medication exposures, and DXA-derived T-scores were extracted from the electronic health record. T-scores above 1 were excluded as likely artifacts or documentation errors. FRAX score [23] was also extracted from the EHR.

For survival analysis, each patient's earliest DXA scan was defined as baseline. The outcome was an incident fragility fracture occurring at least 15 days after baseline; fractures within 15 days were treated as prior events. Patients were followed from baseline until an incident fracture or the last documented clinical encounter. The final cohort comprised 11,522 patients, of whom 859 experienced a fracture during follow-up.

Table 2: Participant demographic and clinical characteristics on the NYP/WCM fracture cohort.

Characteristic	Participants, No. (%)		
	All (N=11522)	Fracture (n=859)	No Fracture (n=10663)
Age, mean (SD), y	68.40 (8.75)	72.03 (8.88)	68.11 (8.68)
Body mass index, mean (SD), kg/m^2	25.37 (5.12)	25.48 (5.34)	25.37 (5.11)
Sex			

Continued on next page

Table 2: Participant demographic and clinical characteristics on the NYP/WCM fracture cohort. (Continued)

Characteristic	Participants, No. (%)		
	All (N=11522)	Fracture (n=859)	No Fracture (n=10663)
Female	10527 (91.4)	739 (86.0)	9788 (91.8)
Male	995 (8.6)	120 (14.0)	875 (8.2)
Smoking status			
Never smoker	6777 (58.8)	451 (52.5)	6326 (59.3)
Former smoker	2927 (25.4)	240 (27.9)	2687 (25.2)
Light smoker	17 (0.1)	0 (0.0)	17 (0.2)
Moderate smoker	570 (4.9)	69 (8.0)	501 (4.7)
Heavy smoker	3 (0.0)	0 (0.0)	3 (0.0)
Current smoker	27 (0.2)	1 (0.1)	26 (0.2)
Unknown	1201 (10.4)	98 (11.4)	1103 (10.3)
Alcohol use			
Never drinker	2808 (24.4)	305 (35.5)	2503 (23.5)
Former drinker	13 (0.1)	2 (0.2)	11 (0.1)
Current drinker	86 (0.7)	9 (1.0)	77 (0.7)
Unknown	8615 (74.8)	543 (63.2)	8072 (75.7)
Previous fracture	305 (35.5)	656 (6.2)	
DXA Result			
Lumbar spine (L1–L4) T-score, mean (SD)	-1.09 (1.02)	-1.23 (1.09)	-1.08 (1.01)
Femoral neck T-score, mean (SD)	-1.61 (0.62)	-1.80 (0.68)	-1.60 (0.62)
Total hip T-score, mean (SD)	-1.22 (0.76)	-1.51 (0.82)	-1.20 (0.76)
Comorbidities			
Alzheimer's disease	76 (0.7)	16 (1.9)	60 (0.6)
Ankylosing spondylitis	18 (0.2)	3 (0.3)	15 (0.1)
Asthma	1391 (12.1)	126 (14.7)	1265 (11.9)
Celiac disease	131 (1.1)	13 (1.5)	118 (1.1)
Cirrhosis	244 (2.1)	23 (2.7)	221 (2.1)
Chronic kidney disease	654 (5.7)	85 (9.9)	569 (5.3)
Chronic obstructive pulmonary disease	442 (3.8)	69 (8.0)	373 (3.5)
Crohn's disease	153 (1.3)	12 (1.4)	141 (1.3)
Cushing syndrome	21 (0.2)	4 (0.5)	17 (0.2)
Eating disorder	54 (0.5)	7 (0.8)	47 (0.4)
Hyperparathyroidism	638 (5.5)	35 (4.1)	603 (5.7)
Hypogonadism	157 (1.4)	16 (1.9)	141 (1.3)
Menopause	772 (6.7)	36 (4.2)	736 (6.9)
Multiple myeloma	125 (1.1)	18 (2.1)	107 (1.0)
Parkinson's disease	85 (0.7)	20 (2.3)	65 (0.6)
Rheumatoid arthritis	401 (3.5)	46 (5.4)	355 (3.3)
Systemic lupus erythematosu	109 (0.9)	8 (0.9)	101 (0.9)

Continued on next page

Table 2: Participant demographic and clinical characteristics on the NYP/WCM fracture cohort. (Continued)

Characteristic	Participants, No. (%)		
	All (N=11522)	Fracture (n=859)	No Fracture (n=10663)
Stroke	463 (4.0)	71 (8.3)	392 (3.7)
Type 1 diabetes	122 (1.1)	11 (1.3)	111 (1.0)
Type 2 diabetes	1737 (15.1)	172 (20.0)	1565 (14.7)
Ulcerative colitis	184 (1.6)	20 (2.3)	164 (1.5)
Medications			
Abaloparatide	139 (1.2)	27 (3.1)	112 (1.1)
Antiandrogens	34 (0.3)	3 (0.3)	31 (0.3)
Antiretrovirals	772 (6.7)	61 (7.1)	711 (6.7)
Aromatase inhibitors	1035 (9.0)	55 (6.4)	980 (9.2)
Bisphosphonates	1760 (15.3)	179 (20.8)	1581 (14.8)
Calcineurin inhibitors	1156 (10.0)	104 (12.1)	1052 (9.9)
Denosumab	506 (4.4)	41 (4.8)	465 (4.4)
Enzyme-inducing antiepileptic drugs	141 (1.2)	19 (2.2)	122 (1.1)
Gonadotropin-releasing hormone agonist/antagonist	281 (2.4)	30 (3.5)	251 (2.4)
Romosozumab	33 (0.3)	3 (0.3)	30 (0.3)
Systemic steroids	2650 (23.0)	262 (30.5)	2388 (22.4)
Teriparatide	139 (1.2)	27 (3.1)	112 (1.1)

2.3 Natural-language conversion of tabular variables

To adapt structured tabular data for LLM input, each variable was converted into a natural-language statement using the template “{column} is {value}” [9, 24]. The covariates used for each cohort are listed in eTable 4 and eTable 5 in Supplement A, respectively.

Statements were concatenated using semicolons. An example of the input is: “Age is 79; Gender is FEMALE; T-score (NECK AVG) category is Osteopenia; Osteoporosis-related disease count is 0; Previous fracture is no”. Domain-specific terminology is explained at the beginning of the prompt to ensure interpretability.

This approach preserves variable identity and value explicitly while presenting the input in a form directly consumable by the language model [8].

2.4 Pairwise ranking formulation for censored survival analysis

Each subject was represented as a tuple (x_i, e_i, t_i) , where x_i denotes the natural-language input, $e_i \in \{0, 1\}$ indicates event occurrence and t_i denotes event or censoring time. Training pairs were constructed from comparable pairs (i, j) , defined as those in which subject i experienced the event ($e_i = 1$) and did so before subject j ’s follow-up time:

$$\mathcal{P} = \{(i, j) \mid e_i = 1, t_i < t_j\}. \quad (1)$$

For each pair, the model was trained to predict which subject would experience the event earlier. This corresponds to learning relative risk ranking rather than absolute survival time. The probability assigned to the model’s chosen next token served as the comparison score r , and supervised fine-tuning optimized a

binary cross-entropy objective over valid comparable pairs.

$$\mathcal{L}_{\text{rank}} = - \sum_{(i,j) \in \mathcal{P}} \log P(r_i > r_j). \quad (2)$$

Because the number of valid pairs can be large, we used a **nested case-control sampling strategy** [25, 26]. For each event case, we randomly selected N subjects with longer follow-up times. The optimal value of N was determined by the model’s performance on the development set.

2.5 Prompt design

For ICU mortality prediction, prompts described two patients and asked the model to decide which patient was expected to die first (Box 1). For fracture prediction, prompts similarly described two patients and asked which was expected to sustain a fracture first, with brief explanations of domain-specific variables included at the beginning of the prompt (Box 2). During training and testing, subject order within prompts was randomized to reduce positional bias.

Box 1: Prompt used for ICU mortality prediction on MIMIC-ICU
You are a genius ICU specialist. You are given descriptions of two patients. Your task is to decide which of them is expected to decrease first:
a. [INSTANCE 1]
b. [INSTANCE 2]
Please provide your answer (a or b).

Box 2: Prompt used for fracture risk assessment on NYP/WCM Fracture
You are a genius orthopedic specialist. Below are descriptions of the relevant terminologies:
<ul style="list-style-type: none"> • Previous fracture: Whether the patient has had a prior fracture. • Osteoporosis-related disease count: The count of comorbidities that increase fracture risk (e.g., rheumatoid arthritis, COPD).
You are given descriptions of two patients. Your task is to decide which of them is expected to sustain a fracture first:
a. [INSTANCE 1]
b. [INSTANCE 2]
Please provide your answer (a or b).

2.5.1 Inference via anchor comparison

In inference, the risk for a test subject was estimated by comparison against a fixed set of anchors sampled from the training cohort. Let $A = \{a_k\}_{k=1}^K$ denote the anchor set [27]. For each anchor a_k , the model predicted whether the test subject s would experience the event earlier than the anchor. This comparison then reduces to a binary decision using a threshold of 0.5:

$$\hat{y}(s, a_k) = \begin{cases} 1, & \text{if } P(r_s, r_{a_k}) > 0.5, \\ 0, & \text{otherwise.} \end{cases} \quad (3)$$

The final risk score was then computed as the proportion of anchors for which the test subject was ranked as higher risk:

$$\hat{r}(s) = \frac{1}{K} \sum_{k=1}^K \hat{y}(s, a_k). \quad (4)$$

In the primary experiments, we set $K = 50$. A higher score indicates greater predicted risk.

2.6 Model backbones and training

We evaluated two locally deployable instruction-tuned LLMs: Llama 3.1-8B-Instruct [28] and Qwen 2.5-7B-Instruct [29]. Fine-tuning was performed on a single A100 GPU without parameter-efficient fine-tuning (PEFT). Based on development-set behavior, the ICU mortality model was fine-tuned for 1 epoch, and the fracture model for 2 epochs. During inference, the temperature was set to a near-zero value (i.e., 0.00001) to produce deterministic outputs.

2.7 Baseline methods

We compared LLMSurvival against conventional and deep survival baselines, including Cox proportional hazards model, Cox-nnet [17], Deephit [18], and DeepSurv [19].

We also compared against task-specific clinical scores: SAPS-II for ICU mortality [22] and FRAX for fracture risk [23, 30].

2.8 Evaluation metrics and statistical analysis

Performance was assessed using the concordance index (C-index) and area under the receiver operating characteristic curve (AUC) at clinically relevant time horizons. The C-index was computed over all comparable pairs in the test set. AUC was calculated by thresholding predicted risk scores to classify event occurrence within each specified time horizon [31].

Confidence intervals were estimated using 1,000 bootstrap resamples. Kaplan–Meier curves were generated on the test set after stratifying individuals into high- and low-risk groups using the median predicted risk from the training cohort.

3 RESULTS

3.1 LLMSurvival reformulates censored survival prediction as a language-based comparison

LLMSurvival comprises three stages (Figure 1a). First, structured covariates are transformed into natural-language descriptions using a standardized template. Second, survival prediction is reformulated as a pairwise ranking task. The LLM is fine-tuned on comparable subject pairs to decide which subject is expected to experience the event earlier. Third, at inference, each test subject is compared with a set of training anchors, and the fraction of comparisons in which the test subject is ranked at higher risk is used as the final risk score (See Section 2: Methods).

This formulation offers two key advantages. First, it naturally incorporates all valid comparable pairs, including those involving censored observations, in a manner consistent with the rationale underlying the concordance index (C-index). Second, identifying which of two subjects experiences the event first is often more intuitive and better defined than directly estimating survival probabilities [15]. This pairwise perspective also aligns with the core assumption of the Cox proportional hazards model: that the relative risk, or hazard ratio, between subjects remains constant over time.

We used Llama 3.1-8B-Instruct as the primary backbone model and evaluated Qwen 2.5-7B-Instruct in parallel. We applied the same framework to two distinct clinical settings (Figure 1b): ICU mortality prediction in MIMIC-IV [32] and fragility fracture prediction in the NYP/WCM fracture cohort. These tasks span markedly different time horizons and disease dynamics, providing a stringent test of generalizability.

3.2 LLMSurvival improves discrimination for ICU mortality prediction

We first assess LLMSurvival on short-term ICU mortality prediction [33]. Prognostic scoring in critical care commonly relies on structured demographic, physiologic, and laboratory variables summarized by systems

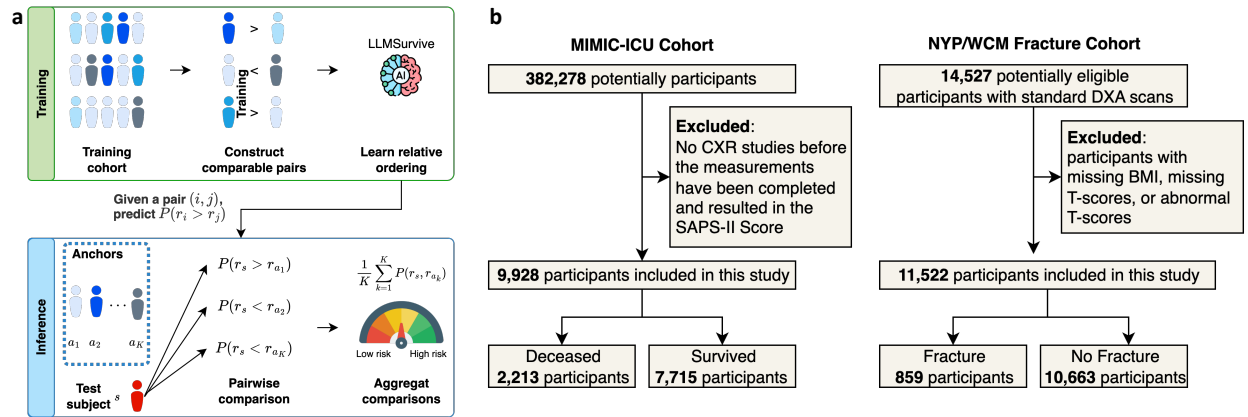


Fig 1: LLMSurvival overview and study cohorts. **a**, Schematic of LLMSurvival. During training, the large language model is fine-tuned on comparable patient pairs to learn the relative ordering of survival times. During inference, each test patient is compared against a fixed set of anchor patients from the training cohort, and the aggregated outcomes define a final risk score. **b**, Cohort construction for the two clinical tasks: ICU mortality prediction in MIMIC-ICU and fracture risk assessment in the NYP/WCM fracture cohort.

such as SAPS II [22].

In MIMIC-ICU, LLMSurvival consistently outperformed conventional survival models (Figure 2a; eTable 2 in Supplement A). Using Llama, LLMSurvival achieved an overall C-index of 0.776 (95% confidence interval [CI], 0.752–0.800), compared with 0.753 (0.726–0.779) for the Cox proportional hazards model, 0.770 (0.744–0.796) for Cox-nnet, 0.730 (0.701–0.756) for DeepHit, and 0.766 (0.739–0.791) for DeepSurv. This corresponds to a 3.0 percentage-point improvement over the established clinical risk tool SAPS-II (0.746 [0.719–0.774]). Using Qwen as the backbone yielded an overall C-index of 0.784 (0.761–0.807), indicating that the framework is robust across LLM families (eTable 2 in Supplement A).

Time-specific analyses showed similar trends. LLMSurvival achieved strong AUC values at 1 day, 2 days, 7 days, and overall, remaining above SAPS-II and competitive with or better than deep survival baselines across all horizons.

These results suggest that the pairwise-ranking formulation captures clinically relevant short-term deterioration in critically ill patients more effectively than conventional survival modeling approaches trained on the same structured inputs.

3.3 LLMSurvival shows robust overall performance for fracture risk prediction

We next evaluated LLMSurvival for fragility fracture prediction using the NYP/WCM cohort (Figure 2b; eTable 3 in Supplement A). Fracture prediction is a longer-horizon task with lower event frequency and a distinct set of clinically relevant covariates, providing a complementary test of the framework [34–37].

In this setting, LLMSurvival again achieved strong discrimination. Using Llama, LLMSurvival reached an overall C-index of 0.742 (0.699–0.783), compared with 0.737 (0.694–0.782) for Cox, 0.684 (0.632–0.728) for Cox-nnet, 0.729 (0.681–0.773) for DeepHit, and 0.730 (0.682–0.772) for DeepSurv. This corresponds to an 8.2 percentage-point improvement over the established clinical reference standard FRAX with a C-index of 0.660 (0.614–0.701) at year 10 [23, 30].

Time-specific AUC analysis showed that LLMSurvival consistently outperformed FRAX across 2-, 3-, and 5-year horizons and surpassed Cox and Cox-nnet at multiple time points. Performance was comparable to DeepSurv overall. Results obtained with Qwen were similar to those obtained with Llama, further support-

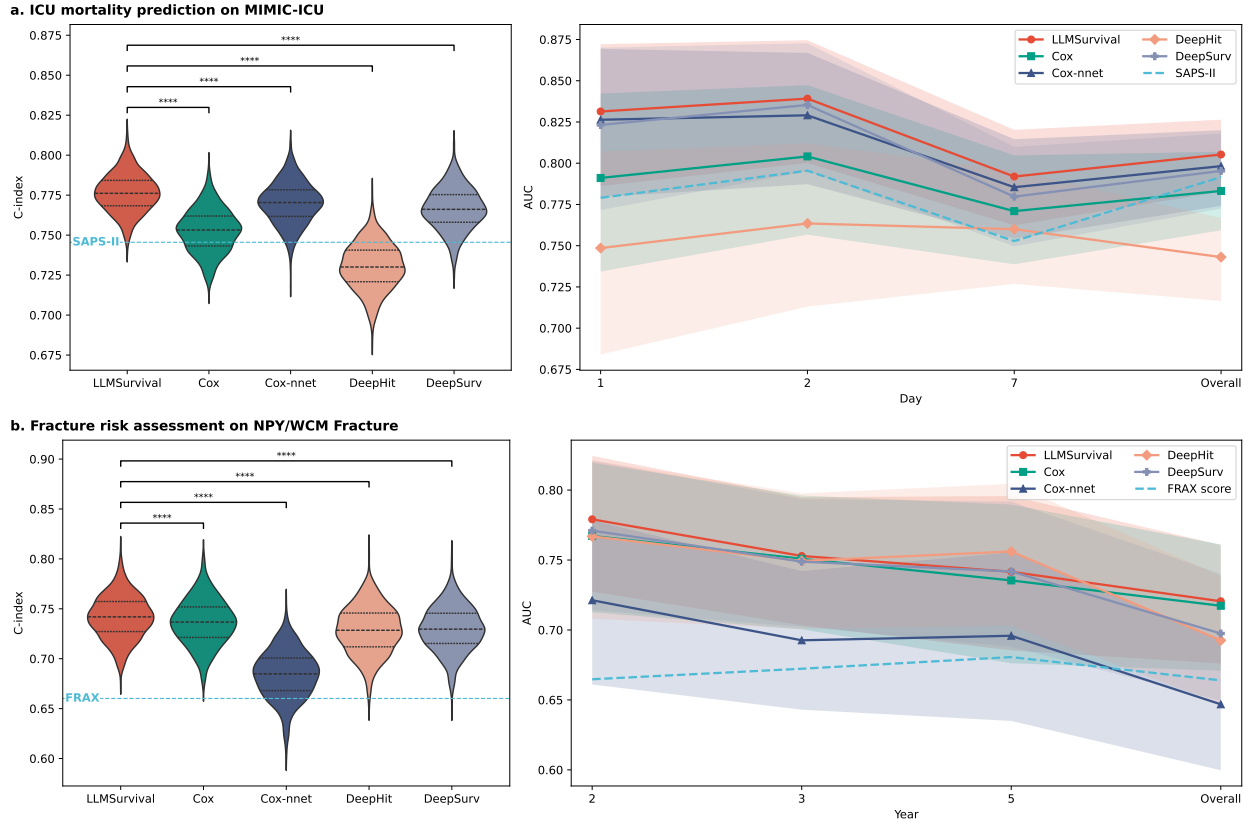


Fig 2: Prognostic performance of LLMSurvival across acute and chronic clinical settings. **a.** ICU mortality prediction on MIMIC-ICU. **b.** Fracture risk assessment in the NYP/WCM fracture cohort. The left panels show distributions of overall C-index values for LLMSurvival, Cox, Cox-nnet, DeepHit, and DeepSurv, with SAPS-II or FRAX indicated by horizontal dashed lines. The right panels show time-specific AUC values across clinically relevant follow-up horizons and overall evaluation. Shaded regions indicate 95% confidence intervals. Statistical annotations are shown for significant comparisons only (**** $p < 0.0001$).

ing backbone robustness (eTable 3 in Supplement A).

Together with the ICU results, these findings indicate that LLMSurvival generalizes across both acute and chronic clinical prediction tasks without task-specific architecture changes.

3.4 LLMSurvival risk scores stratify patients into distinct survival groups

To evaluate clinical usefulness beyond summary discrimination metrics, we examined Kaplan–Meier survival curves for groups defined by LLMSurvival-predicted risk. In each task, participants in the test set were split into high- and low-risk groups based on the median risk score derived from the training cohort.

In both ICU mortality and fracture prediction, LLMSurvival produced clear separation between groups over time (Figure 3). For ICU mortality, the hazard ratio comparing high-risk with low-risk groups was 4.80 (95% CI, 3.74–6.15; $P < 0.005$). For fracture prediction, the hazard ratio was 4.02 (95% CI, 2.75–5.87; $P < 0.005$). These results indicate that LLMSurvival risk scores define clinically meaningful strata with distinct event trajectories.

3.5 Effect of low-to-high risk ratio and anchor count on implementation choices

We next examined two implementation choices that influence LLMSurvival performance. First, we varied the ratio of low-risk to high-risk participants used during pairwise fine-tuning. Increasing the number of low-

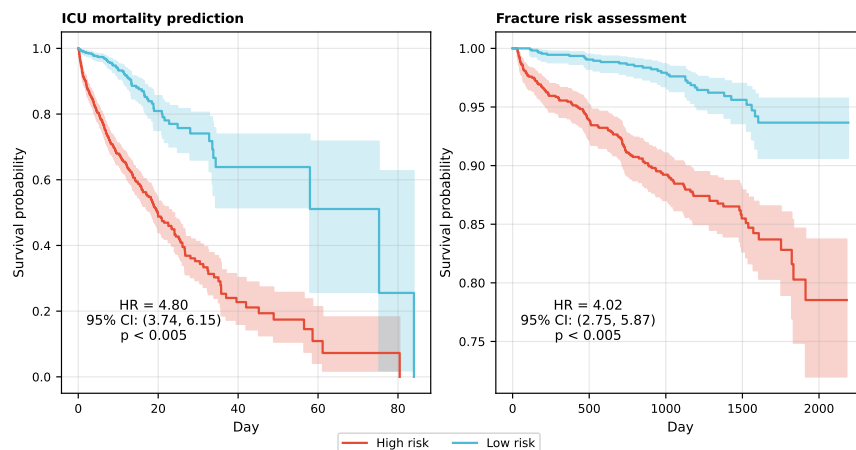


Fig 3: Kaplan–Meier survival curves stratified by LLMSurvival risk score. Participants were stratified into high- and low-risk groups using the median predicted risk score derived from the training cohort. Kaplan–Meier curves were computed on the held-out test set for ICU mortality prediction and fracture risk assessment. Hazard ratios, 95% confidence intervals, and significance values are shown.

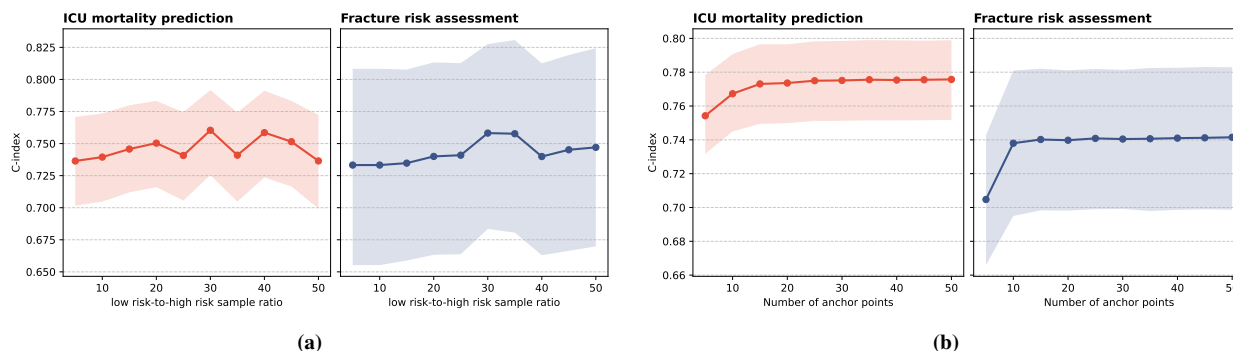


Fig 4: Effect of two implementation choices in LLMSurvival. **a**, Effect of the low-to-high risk ratio during model training. **b**, Effect of anchor count during inference. Shaded bands indicate 95% confidence intervals.

risk samples initially improved performance, indicating stronger ranking supervision, but gains plateaued and then declined at higher ratios (Figure 4a). This pattern was observed across tasks, suggesting that moderate case-control sampling offers a favorable trade-off between signal and noise.

Second, we varied the number of anchor points used during inference. As expected, increasing anchor count improved the stability of risk estimation and increased C-index values initially, after which performance saturated (Figure 4b). In the primary experiments, we used 50 anchors.

We also evaluated alternate anchor-selection and subject-ordering strategies. Differences in C-index were minimal when anchors were drawn randomly versus from positive cases only, and results were stable to pair order in prompts, indicating that LLMSurvival is relatively robust to these procedural variations (eSection A.1 and eSection A.2 in Supplement A).

3.6 Illustrative examples support clinically coherent comparative reasoning

To examine whether pairwise predictions aligned with plausible clinical reasoning, we generated explanatory outputs for representative patient pairs using the base LLMs conditioned on the fine-tuned ranking outcomes (Figure 5). In ICU mortality prediction, the models highlighted clinically meaningful differences

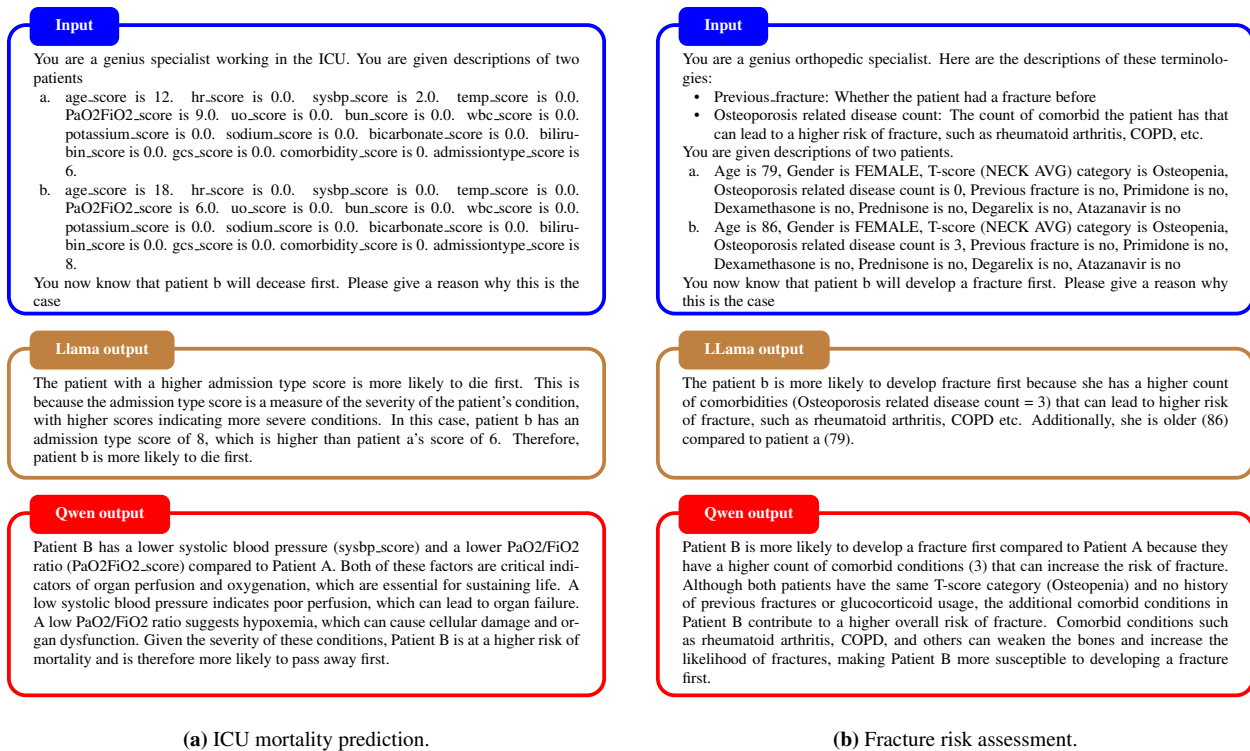


Fig 5: Illustrative examples of generated explanations for pairwise predictions. a, ICU mortality prediction. b, Fracture risk assessment. Outputs are shown for Llama- and Qwen-based models and highlight clinically meaningful differences between patient profiles.

related to admission severity, oxygenation, and blood pressure. In fracture prediction, the models emphasized older age and a higher burden of osteoporosis-related comorbidity.

These examples do not establish causal interpretability, but they suggest that LLMSurvival’s comparison-based outputs can be accompanied by coherent, human-readable rationales grounded in known clinical risk factors.

4 DISCUSSION

We developed LLMSurvival, a framework that enables end-to-end survival analysis with LLMs while accounting for censoring. By converting time-to-event prediction into pairwise ranking over comparable subjects, LLMSurvival resolves a key barrier that has limited direct use of LLMs for survival modeling: the absence of explicit labels for censored observations. This formulation also aligns with a core strength of language models, namely comparative reasoning over textual descriptions.

The framework can be deployed locally because the base models used in our experiments (specifically 7B and 8B variants) are publicly available and relatively small. This architecture mitigates privacy risks by eliminating the need for external API calls.

Across two clinical tasks with markedly different time scales and event profiles, the framework achieved robust overall discrimination and exceeded established clinical scores. In ICU mortality prediction, it outperformed Cox proportional hazards modeling and SAPS-II. In fracture prediction, it exceeded Cox and FRAX and remained competitive with deep survival models. These results suggest that LLMs can function as the primary model for structured survival prediction rather than solely as feature encoders.

An important feature of the framework is its portability. The same general pipeline was applied to an acute critical care task and a chronic fracture risk task without architectural customization. Importantly, LLMSurvival achieves discrimination exceeding established clinical risk scores developed through decades of expert-driven design (SAPS-II for ICU mortality and FRAX for fracture risk). These reference scores are based on manually curated variables and fixed weighting schemes. In contrast, LLMSurvival learns meaningful risk stratification solely from data, as evidenced by clear separation of high- and low-risk groups in the Kaplan–Meier analyses. These results highlight the clinical relevance of LLM-based survival models as flexible alternatives to traditional scoring systems.

More broadly, this work illustrates how reformulating a statistically challenging problem into a task aligned with LLM capabilities can extend the applicability of language models in biomedical machine learning.

This study has several limitations. First, training exhibited some variability across sampling configurations, indicating room for improved optimization stability. Second, pair selection was based on random sampling of comparable controls, and more structured sampling strategies may improve efficiency or performance. Third, inference requires multiple pairwise comparisons against anchors, which introduces additional computational cost. Finally, our experiments used structured tabular inputs only; future work should evaluate the integration of multimodal signals such as clinical notes and medical imaging.

5 CONCLUSION

In summary, LLMSurvival establishes a proof of concept for end-to-end censoring-aware survival analysis with LLMs. The findings support comparison-based reformulation as a practical route for adapting LLMs to censored clinical prediction tasks.

REPRODUCIBILITY

Both Llama- and Qwen-based versions of LLMSurvival showed similar trends across tasks. Additional analyses indicated that performance was relatively insensitive to anchor-selection strategy and robust to pair ordering.

ACKNOWLEDGEMENTS

This research was supported by the National Library of Medicine under the grant numbers R01LM014306, R01LM014344, R01LM014573, R21EY035296 (Y.P.).

ETHICS APPROVAL

This study was approved by the Institutional Review Board of Weill Cornell Medicine (IRB Approval No. 2402027008)

AUTHOR CONTRIBUTIONS

Study concepts/study design, Y.W., H.D., Y.P.; manuscript drafting or manuscript revision for important intellectual content, Y.W., H.D., Y.P.; agrees to ensure any questions related to the work are appropriately resolved, Y.W., H.D., Y.Lin, J.Q., Y.Liu, Y.P.; literature research, Y.W., H.D.; experimental studies, Y.W., H.D., Y.Lin; data interpretation and statistical analysis, Y.W., H.D., J.Q., Y.Liu; and manuscript editing, Y.W., H.D., Y.P.; read and approval of final version of the submitted manuscript, all authors.

COMPETING INTERESTS

None declared.

DATA AVAILABILITY

The MIMIC-ICU dataset used in this study is available from PhysioNet at <https://physionet.org/content/mimiciv>. Access to the NYP/WCM fracture cohort is subject to institutional review and data-sharing restrictions to protect patient privacy and comply with intellectual property obligations. Requests for academic use will be evaluated on a case-by-case basis and may require a material transfer agreement.

CODE AVAILABILITY

Code supporting this study is available for academic research use at <https://github.com/bionlp1ab/llmsurvival>.

REFERENCES

- [1] Ching-Fan Chung, Peter Schmidt, and Ana D Witte. Survival analysis: A survey. *J. Quant. Criminol.*, 7(1):59–98, March 1991. ISSN 0748-4518,1573-7799. doi: 10.1007/bf01083132.
- [2] Vincent Jeanselme, Nikita Agarwal, and Chen Wang. Review of language models for survival analysis. In *AAAI 2024 Spring Symposium on Clinical Foundation Models*, 2024.
- [3] Muhammad Faisal Shahid, Asad Afzal, Abdullah Faiz, Muhammad Siddiqui, Arbaz Khan Shehzad, Fatima Aftab, Muhammad Usamah Shahid, and Muddassar Farooq. Leveraging large language models and survival analysis for early prediction of chemotherapy outcomes. *arXiv preprint arXiv:2603.11594*, 2026.
- [4] Jyothi Vaidyanathan, Shourya Gupta, Justin Lee, Srikanth Prabhu, and Saptarshi Sengupta. Survival analysis for cancers of the brain, cns and bone using retrieval augmented generation on the seer database. In *Proceedings of the AAAI Symposium Series*, volume 5, pages 31–36, 2025.
- [5] Bao Wen, Aihui Wen, Wentian Fang, and Jining Li. Llm-enhanced survival model for electric device lifespan estimation. In *2024 IEEE Smart World Congress (SWC)*, pages 2547–2552. IEEE, 2024.
- [6] Ethan Steinberg, Jason Alan Fries, Yizhe Xu, and Nigam Shah. MOTOR: A time-to-event foundation model for structured medical records. In *The Twelfth International Conference on Learning Representations*, 13 October 2023.
- [7] Aurora Esteban, Victor Cobilean, and Rashmika Nawaratne. Predictive maintenance with large language models and transformer-based survival analysis. In *IECON 2024 - 50th Annual Conference of the IEEE Industrial Electronics Society*, pages 1–6. IEEE, 3 November 2024. ISBN 9781665464543,9781665464550. doi: 10.1109/iecon55916.2024.10905382.
- [8] Tuan Dinh, Yuchen Zeng, Ruisu Zhang, Ziqian Lin, Michael Gira, Shashank Rajput, Jy-Yong Sohn, Dimitris Papailiopoulos, and Kangwook Lee. LIFT: language-interfaced fine-tuning for non-language machine learning tasks. In *Proceedings of the 36th International Conference on Neural Information Processing Systems*, number Article 855 in NIPS '22, pages 11763–11784, Red Hook, NY, USA, 28 November 2022. Curran Associates Inc. ISBN 9781713871088. doi: 10.5555/3600270.3601125.
- [9] Stefan Hegselmann, Alejandro Buendia, Hunter Lang, Monica Agrawal, Xiaoyi Jiang, and David Sontag. TabLLM: Few-shot classification of tabular data with large language models. In *International Conference on Artificial Intelligence and Statistics*, pages 5549–5581. PMLR, 11 April 2023.
- [10] Ping Wang, Yan Li, and Chandan K Reddy. Machine learning for survival analysis: A survey. *ACM Comput. Surv.*, 51(6):1–36, 30 November 2019. ISSN 0360-0300,1557-7341. doi: 10.1145/3214306.
- [11] Bingzhong Jing, Tao Zhang, Zixian Wang, Ying Jin, Kuiyuan Liu, Wenze Qiu, Liangru Ke, Ying Sun, Caisheng He, Dan Hou, Linqun Tang, Xing Lv, and Chaofeng Li. A deep survival analysis method based on ranking. *Artif. Intell. Med.*, 98:1–9, July 2019. ISSN 0933-3657,1873-2860. doi: 10.1016/j.artmed.2019.06.001.
- [12] Vanya Van Belle, Kristiaan Pelckmans, Sabine Van Huffel, and Johan A K Suykens. Support vector methods for survival analysis: a comparison between ranking and regression approaches. *Artif. Intell. Med.*, 53(2):107–118, October 2011. ISSN 0933-3657,1873-2860. doi: 10.1016/j.artmed.2011.06.006.
- [13] Margaux Luck, Tristan Sylvain, Joseph Paul Cohen, Heloise Cardinal, Andrea Lodi, and Yoshua Bengio. Learning to rank for censored survival data. *arXiv preprint arXiv:1806.01984*, 2018.
- [14] Bingzhong Jing, Tao Zhang, Zixian Wang, Ying Jin, Kuiyuan Liu, Wenze Qiu, Liangru Ke, Ying Sun, Caisheng He, Dan Hou, et al. A deep survival analysis method based on ranking. *Artificial intelligence in medicine*, 98:1–9, 2019.

- [15] Zhen Qin, Rolf Jagerman, Kai Hui, Honglei Zhuang, Junru Wu, Le Yan, Jiaming Shen, Tianqi Liu, Jialu Liu, Donald Metzler, Xuanhui Wang, and Michael Bendersky. Large language models are effective text rankers with pairwise ranking prompting. In *Findings of the Association for Computational Linguistics: NAACL 2024*, Stroudsburg, PA, USA, 2024. Association for Computational Linguistics. doi: 10.18653/v1/2024.findings-naacl.97.
- [16] Wen-Shuo Chao, Zhi Zheng, Hengshu Zhu, and Hao Liu. Make large language model a better ranker. In *Findings of the Association for Computational Linguistics: EMNLP 2024*, pages 918–929, Stroudsburg, PA, USA, November 2024. Association for Computational Linguistics. doi: 10.18653/v1/2024.findings-emnlp.51.
- [17] Travers Ching, Xun Zhu, and Lana X Garmire. Cox-nnet: an artificial neural network method for prognosis prediction of high-throughput omics data. *PLoS computational biology*, 14(4):e1006076, 2018.
- [18] Changhee Lee, William Zame, Jinsung Yoon, and Mihaela Van Der Schaar. Deephit: A deep learning approach to survival analysis with competing risks. In *Proceedings of the AAAI conference on artificial intelligence*, volume 32, 2018.
- [19] Jared L Katzman, Uri Shaham, Alexander Cloninger, Jonathan Bates, Tingting Jiang, and Yuval Kluger. DeepSurv: personalized treatment recommender system using a cox proportional hazards deep neural network. *BMC medical research methodology*, 18(1):24, 2018.
- [20] Alistair E W Johnson, Lucas Bulgarelli, Lu Shen, Alvin Gayles, Ayad Shammout, Steven Horng, Tom J Pollard, Sicheng Hao, Benjamin Moody, Brian Gow, Li-Wei H Lehman, Leo A Celi, and Roger G Mark. MIMIC-IV, a freely accessible electronic health record dataset. *Sci. Data*, 10(1):1, 3 January 2023. ISSN 2052-4463. doi: 10.1038/s41597-022-01899-x.
- [21] Mingquan Lin, Song Wang, Ying Ding, Lihui Zhao, Fei Wang, and Yifan Peng. An empirical study of using radiology reports and images to improve ICU-mortality prediction. *IEEE Int. Conf. Healthc. Inform.*, 2021:497–498, August 2021. doi: 10.1109/ichi52183.2021.00088.
- [22] J R Le Gall. A new simplified acute physiology score (SAPS II) based on a european/north american multicenter study. *JAMA*, 270(24):2957–2963, 22 December 1993. ISSN 0098-7484,1538-3598. doi: 10.1001/jama.270.24.2957.
- [23] J.A. Kanis, O. Johnell, A. Odén, H. Johansson, and E. McCloskey. Frax and the assessment of fracture probability in men and women from the uk. *Osteoporosis International*, 19(4):385–397, 2008. doi: 10.1007/s00198-007-0543-5.
- [24] Xi Fang, Weijie Xu, Fiona Anting Tan, Ziqing Hu, Jiani Zhang, Yanjun Qi, Srinivasan H Sengamedu, and Christos Faloutsos. Large language models (LLMs) on tabular data: Prediction, generation, and understanding - a survey. *Transactions on Machine Learning Research*, 2024. ISSN 2835-8856.
- [25] F D K Liddell, J C McDonald, D C Thomas, and Stella V Cunliffe. Methods of cohort analysis: Appraisal by application to asbestos mining. *J. R. Stat. Soc. Ser. A*, 140(4):469, 1977. ISSN 0035-9238,2397-2327. doi: 10.2307/2345280.
- [26] Larry Goldstein and Bryan Langholz. Asymptotic theory for nested case-control sampling in the cox regression model. *Ann. Stat.*, 20(4):1903–1928, 1 December 1992. ISSN 0090-5364,2168-8966. doi: 10.1214/aos/1176348895.
- [27] Yu Liu, Weiyao Tao, Tong Xia, Simon Knight, and Tingting Zhu. SurvUnc: A meta-model based uncertainty quantification framework for survival analysis. In *Proceedings of the 31st ACM SIGKDD Conference on Knowledge Discovery and Data Mining V.2*, pages 1903–1914, New York, NY, USA, 3 August 2025. ACM. doi: 10.1145/3711896.3737140.

[28] Aaron Grattafiori, Abhimanyu Dubey, Abhinav Jauhri, Abhinav Pandey, Abhishek Kadian, Ahmad Al-Dahle, Aiesha Letman, Akhil Mathur, Alan Schelten, Alex Vaughan, Amy Yang, Angela Fan, Anirudh Goyal, Anthony Hartshorn, Aobo Yang, Archi Mitra, Archie Sravankumar, Artem Korenev, Arthur Hinsvark, Arun Rao, Aston Zhang, Aurelien Rodriguez, Austen Gregerson, Ava Spataru, Baptiste Roziere, Bethany Biron, Binh Tang, Bobbie Chern, Charlotte Caucheteux, Chaya Nayak, Chloe Bi, Chris Marra, Chris McConnell, Christian Keller, Christophe Touret, Chunyang Wu, Corinne Wong, Cristian Canton Ferrer, Cyrus Nikolaidis, Damien Allonsius, Daniel Song, Danielle Pintz, Danny Livshits, Danny Wyatt, David Esiobu, Dhruv Choudhary, Dhruv Mahajan, Diego Garcia-Olano, Diego Perino, Dieuwke Hupkes, Egor Lakomkin, Ehab AlBadawy, Elina Lobanova, Emily Dinan, Eric Michael Smith, Filip Radenovic, Francisco Guzmán, Frank Zhang, Gabriel Synnaeve, Gabrielle Lee, Georgia Lewis Anderson, Govind Thattai, Graeme Nail, Gregoire Mialon, Guan Pang, Guillem Cucurell, Hailey Nguyen, Hannah Korevaar, Hu Xu, Hugo Touvron, Iliyan Zarov, Imanol Arrieta Ibarra, Isabel Kloumann, Ishan Misra, Ivan Evtimov, Jack Zhang, Jade Copet, Jaewon Lee, Jan Geffert, Jana Vranes, Jason Park, Jay Mahadeokar, Jeet Shah, Jelmer van der Linde, Jennifer Billock, Jenny Hong, Jenya Lee, Jeremy Fu, Jianfeng Chi, Jianyu Huang, Jiawen Liu, Jie Wang, Jiecao Yu, Joanna Bitton, Joe Spisak, Jongsoo Park, Joseph Rocca, Joshua Johnstun, Joshua Saxe, Junteng Jia, Kalyan Vasuden Alwala, Karthik Prasad, Kartikeya Upasani, Kate Plawiak, Ke Li, Kenneth Heafield, Kevin Stone, Khalid El-Arini, Krithika Iyer, Kshitiz Malik, Kuenley Chiu, Kunal Bhalla, Kushal Lakhotia, Lauren Rantala-Yearly, Laurens van der Maaten, Lawrence Chen, Liang Tan, Liz Jenkins, Louis Martin, Lovish Madaan, Lubo Malo, Lukas Blecher, Lukas Landzaat, Luke de Oliveira, Madeline Muzzi, Mahesh Pasupuleti, Mannat Singh, Manohar Paluri, Marcin Kardas, Maria Tsimpoukelli, Mathew Oldham, Mathieu Rita, Maya Pavlova, Melanie Kambadur, Mike Lewis, Min Si, Mitesh Kumar Singh, Mona Hassan, Naman Goyal, Narjes Torabi, Nikolay Bashlykov, Nikolay Bogoychev, Niladri Chatterji, Ning Zhang, Olivier Duchenne, Onur Çelebi, Patrick Alrassy, Pengchuan Zhang, Pengwei Li, Petar Vasic, Peter Weng, Prajjwal Bhargava, Pratik Dubal, Praveen Krishnan, Punit Singh Koura, Puxin Xu, Qing He, Qingxiao Dong, Ragavan Srinivasan, Raj Ganapathy, Ramon Calderer, Ricardo Silveira Cabral, Robert Stojnic, Roberta Raileanu, Rohan Maheswari, Rohit Girdhar, Rohit Patel, Romain Sauvestre, Ronnie Polidoro, Roshan Sumbaly, Ross Taylor, Ruan Silva, Rui Hou, Rui Wang, Saghar Hosseini, Sahana Chennabasappa, Sanjay Singh, Sean Bell, Seohyun Sonia Kim, Sergey Edunov, Shaoliang Nie, Sharan Narang, Sharath Raparthy, Sheng Shen, Shengye Wan, Shruti Bhosale, Shun Zhang, Simon Vandenhende, Soumya Batra, Spencer Whitman, Sten Sootla, Stephane Collot, Suchin Gururangan, Sydney Borodinsky, Tamar Herman, Tara Fowler, Tarek Sheasha, Thomas Georgiou, Thomas Scialom, Tobias Speckbacher, Todor Mihaylov, Tong Xiao, Ujjwal Karn, Vedanuj Goswami, Vibhor Gupta, Vignesh Ramanathan, Viktor Kerkez, Vincent Gonguet, Virginie Do, Vish Vogeti, Vitor Albiero, Vladan Petrovic, Weiwei Chu, Wenhan Xiong, Wenyin Fu, Whitney Meers, Xavier Martinet, Xiaodong Wang, Xiaofang Wang, Xiaoqing Ellen Tan, Xide Xia, Xinfeng Xie, Xuchao Jia, Xuewei Wang, Yaelle Goldschlag, Yashesh Gaur, Yasmine Babaei, Yi Wen, Yiwen Song, Yuchen Zhang, Yue Li, Yuning Mao, Zacharie Delpierre Coudert, Zheng Yan, Zhengxing Chen, Zoe Papanikos, Aaditya Singh, Aayushi Srivastava, Abha Jain, Adam Kelsey, Adam Shajnfeld, Adithya Gangidi, Adolfo Victoria, Ahuva Goldstand, Ajay Menon, Ajay Sharma, Alex Boesenberg, Alexei Baevski, Allie Feinstein, Amanda Kallet, Amit Sangani, Amos Teo, Anam Yunus, Andrei Lupu, Andres Alvarado, Andrew Caples, Andrew Gu, Andrew Ho, Andrew Poulton, Andrew Ryan, Ankit Ramchandani, Annie Dong, Annie Franco, Anuj Goyal, Aparajita Saraf, Arkabandhu Chowdhury, Ashley Gabriel, Ashwin Barambe, Assaf Eisenman, Azadeh Yazdan, Beau James, Ben Maurer, Benjamin Leonhardi, Bernie Huang, Beth Loyd, Beto De Paola, Bhargavi Paranjape, Bing Liu, Bo Wu, Boyu Ni, Braden Hancock, Bram Wasti, Brandon Spence, Brani Stojkovic, Brian Gamido, Britt Montalvo, Carl Parker, Carly Burton, Catalina Mejia, Ce Liu, Changan Wang, Changkyu Kim, Chao Zhou, Chester Hu, Ching-Hsiang Chu, Chris Cai, Chris Tindal, Christoph Feichtenhofer, Cynthia Gao, Damon Civin, Dana Beaty, Daniel Kreymer, Daniel Li,

David Adkins, David Xu, Davide Testuggine, Delia David, Devi Parikh, Diana Liskovich, Didem Foss, Ding Kang Wang, Duc Le, Dustin Holland, Edward Dowling, Eissa Jamil, Elaine Montgomery, Eleonora Presani, Emily Hahn, Emily Wood, Eric-Tuan Le, Erik Brinkman, Esteban Arcaute, Evan Dunbar, Evan Smothers, Fei Sun, Felix Kreuk, Feng Tian, Filippos Kokkinos, Firat Ozgenel, Francesco Caggioni, Frank Kanayet, Frank Seide, Gabriela Medina Florez, Gabriella Schwarz, Gada Badeer, Georgia Sweet, Gil Halpern, Grant Herman, Grigory Sizov, Guangyi, Zhang, Guna Lakshminarayanan, Hakan Inan, Hamid Shojanazeri, Han Zou, Hannah Wang, Hanwen Zha, Haroun Habeeb, Harrison Rudolph, Helen Suk, Henry Aspegren, Hunter Goldman, Hongyuan Zhan, Ibrahim Damlaj, Igor Molybog, Igor Tufanov, Ilias Leontiadis, Irina-Elena Veliche, Itai Gat, Jake Weissman, James Geboski, James Kohli, Janice Lam, Japhet Asher, Jean-Baptiste Gaya, Jeff Marcus, Jeff Tang, Jennifer Chan, Jenny Zhen, Jeremy Reizenstein, Jeremy Teboul, Jessica Zhong, Jian Jin, Jingyi Yang, Joe Cummings, Jon Carvill, Jon Shepard, Jonathan McPhie, Jonathan Torres, Josh Ginsburg, Junjie Wang, Kai Wu, Kam Hou U, Karan Saxena, Kartikay Khandelwal, Katayoun Zand, Kathy Matosich, Kaushik Veeraraghavan, Kelly Michelen, Keqian Li, Kiran Jagadeesh, Kun Huang, Kunal Chawla, Kyle Huang, Lailin Chen, Lakshya Garg, Lavender A, Leandro Silva, Lee Bell, Lei Zhang, Liangpeng Guo, Licheng Yu, Liron Moshkovich, Luca Wehrstedt, Madian Khabsa, Manav Avalani, Manish Bhatt, Martynas Mankus, Matan Hasson, Matthew Lennie, Matthias Reso, Maxim Groshev, Maxim Naumov, Maya Lathi, Meghan Keneally, Miao Liu, Michael L Seltzer, Michal Valko, Michelle Restrepo, Mihir Patel, Mik Vyatskov, Mikayel Samvelyan, Mike Clark, Mike Macey, Mike Wang, Miquel Jubert Hermoso, Mo Metanat, Mohammad Rastegari, Munish Bansal, Nandhini Santhanam, Natascha Parks, Natasha White, Navyata Bawa, Nayan Singhal, Nick Egebo, Nicolas Usunier, Nikhil Mehta, Nikolay Pavlovich Laptev, Ning Dong, Norman Cheng, Oleg Chernoguz, Olivia Hart, Omkar Salpekar, Ozlem Kalinli, Parkin Kent, Parth Parekh, Paul Saab, Pavan Balaji, Pedro Rittner, Philip Bontrager, Pierre Roux, Piotr Dollar, Polina Zvyagina, Prashant Ratan-chandani, Pritish Yuvraj, Qian Liang, Rachad Alao, Rachel Rodriguez, Rafi Ayub, Raghotham Murthy, Raghu Nayani, Rahul Mitra, Rangaprabhu Parthasarathy, Raymond Li, Rebekkah Hogan, Robin Batten, Rocky Wang, Russ Howes, Ruty Rinott, Sachin Mehta, Sachin Siby, Sai Jayesh Bondu, Samyak Datta, Sara Chugh, Sara Hunt, Sargun Dhillon, Sasha Sidorov, Satadru Pan, Saurabh Mahajan, Saurabh Verma, Seiji Yamamoto, Sharadh Ramaswamy, Shaun Lindsay, Sheng Feng, Shenghao Lin, Shengxin Cindy Zha, Shishir Patil, Shiva Shankar, Shuqiang Zhang, Shuqiang Zhang, Sinong Wang, Sneha Agarwal, Soji Sajuyigbe, Soumith Chintala, Stephanie Max, Stephen Chen, Steve Kehoe, Steve Satterfield, Sudarshan Govindaprasad, Sumit Gupta, Summer Deng, Sungmin Cho, Sunny Virk, Suraj Subramanian, Sy Choudhury, Sydney Goldman, Tal Remez, Tamar Glaser, Tamara Best, Thilo Koehler, Thomas Robinson, Tianhe Li, Tianjun Zhang, Tim Matthews, Timothy Chou, Tzook Shaked, Varun Vontimitta, Victoria Ajayi, Victoria Montanez, Vijai Mohan, Vinay Satish Kumar, Vishal Mangla, Vlad Ionescu, Vlad Poenaru, Vlad Tiberiu Mihalescu, Vladimir Ivanov, Wei Li, Wenchen Wang, Wenwen Jiang, Wes Bouaziz, Will Constable, Xiao Cheng Tang, Xiao Jian Wu, Xiaolan Wang, Xilun Wu, Xinbo Gao, Yaniv Kleinman, Yanjun Chen, Ye Hu, Ye Jia, Ye Qi, Yenda Li, Yilin Zhang, Ying Zhang, Yossi Adi, Youngjin Nam, Yu, Wang, Yu Zhao, Yuchen Hao, Yundi Qian, Yunlu Li, Yuzi He, Zach Rait, Zachary DeVito, Zef Rosnbrick, Zhaoduo Wen, Zhenyu Yang, Zhiwei Zhao, and Zhiyu Ma. The llama 3 herd of models. *arXiv [cs.AI]*, 31 July 2024.

[29] Qwen, An Yang, Baosong Yang, Beichen Zhang, Binyuan Hui, Bo Zheng, Bowen Yu, Chengyuan Li, Dayiheng Liu, Fei Huang, Haoran Wei, Huan Lin, Jian Yang, Jianhong Tu, Jianwei Zhang, Jianxin Yang, Jiayi Yang, Jingren Zhou, Junyang Lin, Kai Dang, Keming Lu, Keqin Bao, Kexin Yang, Le Yu, Mei Li, Mingfeng Xue, Pei Zhang, Qin Zhu, Rui Men, Runji Lin, Tianhao Li, Tianyi Tang, Tingyu Xia, Xingzhang Ren, Xuancheng Ren, Yang Fan, Yang Su, Yichang Zhang, Yu Wan, Yuqiong Liu, Zeyu Cui, Zhenru Zhang, and Zihan Qiu. Qwen2.5 technical report. *arXiv [cs.CL]*, 19 December 2024.

[30] J.A. Kanis, A. Odén, H. Johansson, F. Borgström, O. Ström, and E. McCloskey. Frax and its applica-

- tions to clinical practice. *Bone*, 44(5):734–743, 2009. doi: 10.1016/j.bone.2009.01.373.
- [31] Jin Huang and C X Ling. Using AUC and accuracy in evaluating learning algorithms. *IEEE Trans. Knowl. Data Eng.*, 17(3):299–310, March 2005. ISSN 1041-4347,1558-2191. doi: 10.1109/tkde.2005.50.
- [32] Alistair Johnson, Lucas Bulgarelli, Tom Pollard, Steven Horng, Leo Anthony Celi, and Roger Mark. MIMIC-IV, 2020.
- [33] Angela K M Lipshutz, John R Feiner, Barbara Grimes, and Michael A Gropper. Predicting mortality in the intensive care unit: a comparison of the university health consortium expected probability of mortality and the mortality prediction model III. *J. Intensive Care*, 4(1):35, 23 May 2016. ISSN 2052-0492. doi: 10.1186/s40560-016-0158-z.
- [34] GBD 2019 Fracture Collaborators. Global, regional, and national burden of bone fractures in 204 countries and territories, 1990–2019: a systematic analysis from the global burden of disease study 2019. *The Lancet Healthy Longevity*, 2(9):e580–e592, 2021. doi: 10.1016/S2666-7568(21)00172-0.
- [35] World Health Organization. Fragility fractures, 2024. URL <https://www.who.int/news-room/fact-sheets/detail/fragility-fractures>. Fact sheet, 25 September 2024.
- [36] U.S. Preventive Services Task Force. Osteoporosis to prevent fractures: Screening, 2025. URL <https://uspreventiveservicestaskforce.org/uspstf/recommendation/osteoporosis-screening>. Recommendation statement (Jan 14, 2025).
- [37] W. K. Nicholson et al. Screening for osteoporosis to prevent fractures: Us preventive services task force recommendation statement. *JAMA*, 2025.
- [38] Yifan Zeng, Ojas Tendolkar, Raymond Baartmans, Qingyun Wu, Lizhong Chen, and Huazheng Wang. LLM-RankFusion: Mitigating intrinsic inconsistency in LLM-based ranking. *arXiv [cs.IR]*, 31 May 2024.
- [39] Murray Rosenblatt. Remarks on some nonparametric estimates of a density function. *Annals of Mathematical Statistics*, 27:832–837, 1956.
- [40] Emanuel Parzen. On estimation of a probability density function and mode. *Annals of Mathematical Statistics*, 33:1065–1076, 1962.

A SUPPLEMENT

eTable 1: Summary of previous literature

Author	Model Type	Description of how they tackle survival analysis
Esteban et al. [7]	Deep Learning, LLM	Added dedicated neural networks on top of an LLM and experimented with ordinal regression loss and discordant pair loss.
Jeanselme et al. [2]	LLM (Review)	Reviewed existing literature, observing that most studies utilize LLMs as feature extractors rather than direct predictive models, or require substantial architectural modifications.
Jing et al. [14]	Deep Learning	Tackling the survival analysis problem as a ranking problem in the deep learning Era.
Luck et al. [13]	Deep Learning	Tackling the survival analysis problem as a ranking problem in the deep learning Era.
Shahid et al. [3]	LLM	Used an LLM as a feature extractor to obtain variables from clinical notes.
Steinberg et al. [6]	Deep Learning, LLM	Attached a piecewise exponential artificial neural network on top of a foundation model dedicated to predicting the hazard rate.
Vaidyanathan et al. [4]	LLM	Simplified the survival analysis problem into a five-year classification task and did not address censoring.
Van Belle et al. [12]	Machine Learning	Explored treating survival analysis as a ranking problem using support vector methods.
Wen et al. [5]	LLM	Used an LLM to extract features for a downstream survival model.

eTable 2: Performance comparison for ICU mortality prediction on the MIMIC-ICU cohort.

	Overall (n=1,984)	1 day (n=1,955)	2 day (n=1,885)	7 day (n=1,239)
C-Index				
SAPS II	0.746 (0.719, 0.774)	0.771 (0.724, 0.820)	0.784 (0.742, 0.824)	0.726 (0.695, 0.756)
Cox	0.753 (0.726, 0.779)	0.784 (0.729, 0.834)	0.793 (0.747, 0.835)	0.744 (0.713, 0.775)
Cox-nnet	0.770 (0.744, 0.796)	0.820 (0.774, 0.863)	0.819 (0.778, 0.856)	0.760 (0.730, 0.787)
Deephit	0.730 (0.701, 0.756)	0.743 (0.681, 0.800)	0.755 (0.706, 0.802)	0.733 (0.701, 0.767)
Deepsurv	0.766 (0.739, 0.791)	0.816 (0.766, 0.863)	0.825 (0.786, 0.862)	0.756 (0.727, 0.784)
LLMSurvival (Qwen)	0.784 (0.761, 0.807)	0.832 (0.787, 0.872)	0.841 (0.806, 0.872)	0.772 (0.745, 0.797)
LLMSurvival (Llama)	0.776 (0.752, 0.800)	0.824 (0.779, 0.865)	0.828 (0.791, 0.862)	0.765 (0.737, 0.791)
AUC				
SAPS II	0.792 (0.768, 0.814)	0.779 (0.730, 0.828)	0.795 (0.752, 0.836)	0.753 (0.720, 0.785)
Cox model	0.783 (0.759, 0.807)	0.791 (0.734, 0.842)	0.804 (0.757, 0.847)	0.771 (0.739, 0.805)
Cox-nnet	0.798 (0.774, 0.820)	0.826 (0.779, 0.869)	0.829 (0.787, 0.867)	0.785 (0.754, 0.815)
Deephit	0.743 (0.716, 0.767)	0.749 (0.684, 0.807)	0.763 (0.713, 0.812)	0.760 (0.727, 0.795)
Deepsurv	0.795 (0.773, 0.818)	0.823 (0.772, 0.870)	0.835 (0.795, 0.873)	0.780 (0.750, 0.810)
LLMSurvival (Qwen)	0.809 (0.787, 0.830)	0.839 (0.793, 0.880)	0.853 (0.817, 0.886)	0.797 (0.767, 0.825)
LLMSurvival (Llama)	0.805 (0.783, 0.826)	0.831 (0.786, 0.872)	0.839 (0.800, 0.875)	0.792 (0.762, 0.820)

eTable 3: Performance comparison for fracture risk assessment on the NYP/WCM fracture cohort.

	Overall (n=2,235)	2y (n=1,738)	3y (n=1,244)	5y (n=322)
C-Index				
FRAX	0.660 (0.614, 0.701)	0.659 (0.613, 0.703)	0.661 (0.618, 0.701)	0.622 (0.583, 0.663)
Cox model	0.737 (0.694, 0.782)	0.762 (0.709, 0.813)	0.742 (0.694, 0.785)	0.697 (0.651, 0.739)
Cox-nnet	0.684 (0.632, 0.728)	0.718 (0.659, 0.774)	0.689 (0.642, 0.737)	0.675 (0.630, 0.718)
Deephit	0.729 (0.681, 0.773)	0.763 (0.705, 0.815)	0.743 (0.696, 0.789)	0.723 (0.682, 0.761)
DeepSurv	0.730 (0.682, 0.772)	0.766 (0.711, 0.816)	0.742 (0.697, 0.785)	0.708 (0.666, 0.747)
LLMSurvival (Qwen)	0.741 (0.699, 0.784)	0.772 (0.723, 0.818)	0.745 (0.699, 0.786)	0.705 (0.662, 0.746)
LLMSurvival (Llama)	0.742 (0.699, 0.783)	0.774 (0.723, 0.818)	0.744 (0.696, 0.784)	0.701 (0.657, 0.740)
AUC				
FRAX	0.664 (0.621, 0.704)	0.665 (0.616, 0.710)	0.672 (0.626, 0.715)	0.681 (0.623, 0.735)
Cox model	0.717 (0.671, 0.761)	0.767 (0.713, 0.820)	0.751 (0.700, 0.796)	0.735 (0.676, 0.790)
Cox-nnet	0.647 (0.600, 0.692)	0.721 (0.661, 0.778)	0.693 (0.643, 0.742)	0.696 (0.635, 0.755)
Deephit	0.693 (0.647, 0.739)	0.767 (0.708, 0.821)	0.749 (0.701, 0.798)	0.756 (0.703, 0.804)
DeepSurv	0.697 (0.649, 0.740)	0.771 (0.714, 0.821)	0.749 (0.702, 0.794)	0.742 (0.688, 0.792)
LLMSurvival (Qwen)	0.720 (0.678, 0.761)	0.777 (0.727, 0.825)	0.753 (0.704, 0.796)	0.741 (0.684, 0.795)
LLMSurvival (Llama)	0.721 (0.676, 0.761)	0.779 (0.727, 0.824)	0.753 (0.703, 0.795)	0.742 (0.685, 0.796)

eTable 4: Summary of covariates used for ICU mortality prediction on MIMIC-IV ICU dataset.

Covariate	Description
age_score	Points assigned based on patient age.
hr_score	Heart rate abnormality score.
sysbp_score	Systolic blood pressure abnormality score.
temp_score	Body temperature abnormality score.
PaO2FiO2_score	Oxygenation score based on the PaO ₂ /FiO ₂ ratio.
uo_score	Urine output score reflecting renal perfusion.
bun_score	Blood urea nitrogen abnormality score (renal function).
wbc_score	White blood cell count abnormality score (infection/sepsis).
potassium_score	Serum potassium abnormality score.
sodium_score	Serum sodium abnormality score.
bicarbonate_score	Serum bicarbonate abnormality score (acid–base balance).
bilirubin_score	Serum bilirubin level score (liver dysfunction).
gcs_score	Glasgow Coma Scale score (neurological status).
comorbidity_score	Score derived from chronic health conditions.
admissiontype_score	Points assigned based on admission type.

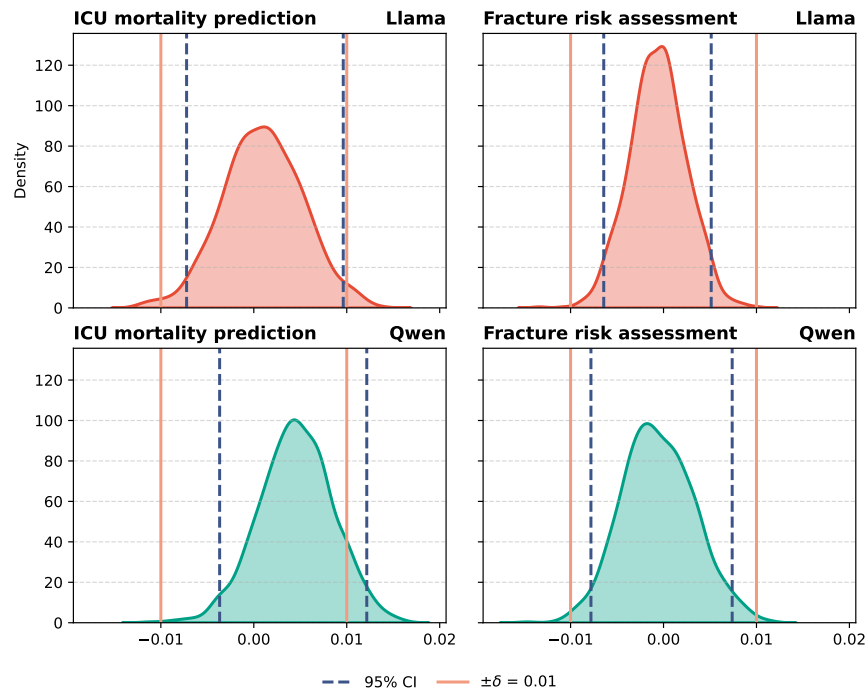
eTable 5: Summary of covariates used for fracture risk assessment on NPY/WCM-fracture dataset

Covariate	Description
Age	Age at baseline.
Sex	Participant's sex
Previous_fracture	Whether the patient has had a prior fracture.
T-score (NECK AVG) category	T-score from the average bone density of the femoral neck, categorized to Normal (above -1), Osteopenia (-2.5 -1.0), and Osteoporosis (below -2.5).
Osteoporosis-related disease count	Count of the 22 diseases listed in Table 2.
Primidone	An anticonvulsant medication used to treat epilepsy and essential tremor.
Dexamethasone	A potent synthetic corticosteroid (steroid) medication used to treat a wide range of inflammatory, autoimmune, and hormonal conditions.
Prednisone	A potent synthetic corticosteroid used to treat inflammatory and autoimmune conditions, ranging from asthma to cancer.
Degarelix	a GnRH antagonist injection for advanced prostate cancer.
Atazanavir	An antiretroviral protease inhibitor for HIV.

A.1 Anchor selection minimally influences risk predictions

We assessed whether anchor-point selection influences risk estimation (eFigure 1). We compared two strategies: (1) random sampling of anchors from the full training set (“random”; primary analysis) and (2) selection of anchors exclusively from event cases (“event-only”). Paired differences in C-index between the two strategies were visualized using kernel density estimation, together with bootstrap confidence intervals and an equivalence bound of $\delta = 0.01$.

Across both tasks, differences were minimal for both Llama- and Qwen-based LLMSurvival. For Llama-based LLMSurvival, the mean differences were 0.0010 (-0.0072, 0.0096) for ICU mortality prediction and -0.0006 (-0.0064, 0.0051) for fracture risk assessment. For Qwen-based LLMSurvival, the corresponding mean differences were 0.0045 (-0.0037, 0.0122) and 0.0031 (-0.0143, 0.0218). Most estimates lie within the equivalence bound, indicating similar performance across anchor-selection strategies. Even when differences slightly exceeded δ , the absolute deviations were negligible, and the confidence intervals remained narrow, supporting the conclusion that anchor selection has little influence on risk estimation.

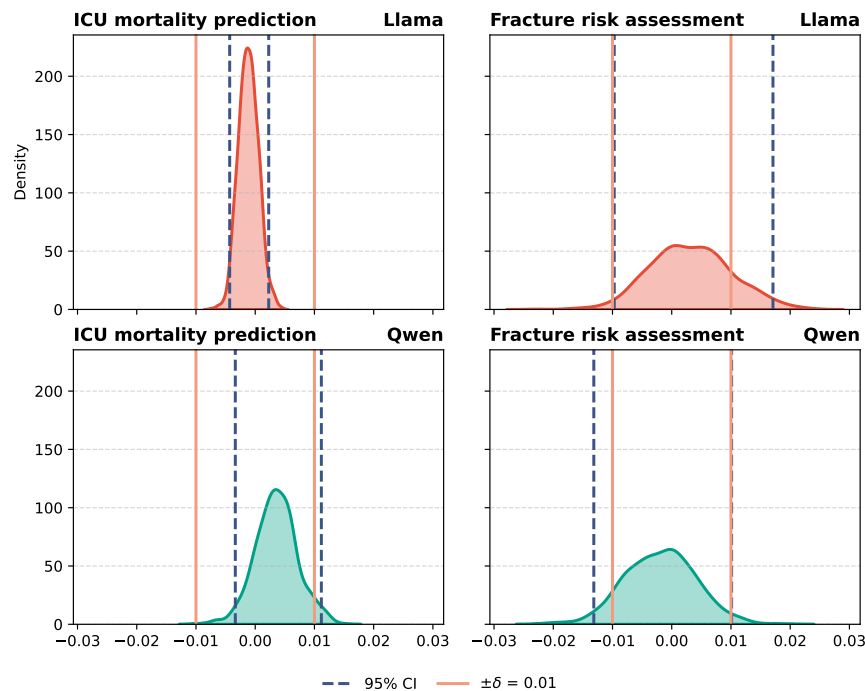


eFigure 1: Comparison of anchor selection strategies for risk estimation. Paired differences in C-index between random anchor selection and event-only anchors (random minus event-only) using LLaMA and Qwen backbones. Kernel density estimation (KDE) curves depict bootstrap distributions of paired differences, with shaded regions indicating 95% confidence intervals. Dashed lines denote equivalence bounds ($\pm\delta = 0.01$).

A.2 LLMSurvival is robust to subject order in LLM ranking

Order inconsistency is a known limitation of LLMs as rankers [15, 38], referring to cases in which reversing the order of subjects in the prompt (for example, “rank A, B” versus “rank B, A”) leads to different outputs. To evaluate the impact of this issue, we compared two prompting strategies: (1) randomly shuffling the target and anchor subjects (“shuffle”; primary analysis) and (2) fixing the anchor in the first position (“fix_a”). Paired differences in C-index between the two strategies were visualized using kernel density estimation (KDE) [39, 40] with bootstrap resampling, together with 95% confidence intervals and an equivalence bound of $\delta = 0.01$ to assess practical significance.

As shown in eFigure 2, differences were minimal across tasks. For Llama-based LLMSurvival, the mean paired differences were -0.0011 (-0.0043, 0.0023) for ICU mortality prediction and 0.0033 [-0.0097, 0.0171] for fracture risk assessment. Relative to the equivalence bound, the difference for ICU mortality fell well within the prespecified threshold, indicating negligible effects of subject ordering. For fracture risk assessment, the estimate slightly exceeded δ , but the absolute deviation remained small. Bootstrap confidence intervals were narrow and centered near zero, supporting comparable performance between the two strategies. Similar patterns were observed for Qwen-based LLMSurvival, with mean paired differences of 0.0036 (-0.0034, 0.0112) and -0.0004 (-0.0192, 0.0106). Overall, these findings suggest that LLMSurvival is robust to subject order, with minimal influence on risk estimation performance.



eFigure 2: Evaluation of order inconsistency in pairwise comparisons. Paired differences in C-index between shuffled and fixed-anchor ordering (shuffle minus fix_a) using LLaMA and Qwen backbones. Kernel density estimation (KDE) curves depict bootstrap distributions of paired differences, with shaded regions indicating 95% confidence intervals. Dashed lines denote equivalence bounds ($\pm\delta = 0.01$).